

# Gas Transport in Polymers Prepared via Metathesis Copolymerization of *exo-N*-Phenyl-7-oxanorbornene-5,6-dicarboximide and Norbornene

Mikhail A. Tlenkopatchev and Joel Vargas

*Instituto de Investigaciones en Materiales, Universidad Autónoma de México, Apartado Postal 70-360 CU, Coyoacán, México DF 04510, México*

María del Mar López-González and Evaristo Riande\*

*Instituto de Ciencia y Tecnología de Polímeros (CSIC), 28006 Madrid, Spain*

Received May 22, 2003; Revised Manuscript Received August 12, 2003

**ABSTRACT:** This work reports the synthesis of *exo-N*-phenyl-7-oxanorbornene-5,6-dicarboximide and its ring-opening metathesis copolymerization with norbornene to yield poly(*exo-N*-phenyl-7-oxanorbornene-5,6-dicarboximide-*co*-norbornene), with molar ratio 50/50. The glass transition temperature of the copolymer is 125 °C. Permeation and sorption processes of different gases (hydrogen, nitrogen, oxygen, carbon monoxide, carbon dioxide, methane, ethylene, and ethane) were measured in membranes prepared by casting from solutions of the copolymer in chloroform. The Langmuir capacity of the gases is relatively small due to the nearness of the glass transition temperature of the polymer to the working temperature. The solution of the most condensable gases in the continuous phase of the membrane is apparently described by the Flory–Huggins theory of polymer–diluent mixtures. In general, the membranes exhibit a reasonably high separation coefficient of hydrogen with respect to ethane, ethylene, nitrogen, and methane. The value of  $\alpha(\text{O}_2/\text{N}_2)$  at room temperature lies in the vicinity of 5.

## Introduction

The ever increasing use of membranes as an alternative to the cryogenic industries for producing nitrogen-enriched air, as well as the use of membrane technology in the petrochemical industry, has encouraged studies of the relationship between structure and transport properties of different classes of polymers.<sup>1,2</sup> Polynorbornene and derivatives have been widely used in the past decade for permeation and sorption studies. Norbornene monomers have been the subject of interest due to facile preparation and functionalization.<sup>3–5</sup> Functionalized norbornenes easily participated in ring-opening metathesis polymerization (ROMP) with approximate complete conversion to high molecular weight polymers with good mechanical properties.<sup>6,7</sup> Some of the polynorbornenes showed very attractive gas transport properties. Thus, fluorine-containing glassy polynorbornene as well as organosilicon-substituted polynorbornene have been synthesized,<sup>8–11</sup> observing in both cases an increase in glass transition temperature and gas permeability. More recently, Steinhäusler and Koros<sup>12</sup> reported that a high order tacticity has a positive effect on both permeation and separation processes. It has also been reported that introduction of tosylate group into the five-membered ring of the polynorbornene main chain resulted in increase of glass transition temperature and significant improvement in selectivity for  $\text{O}_2/\text{N}_2$ .<sup>13</sup> In most cases, however, substituted polynorbornenes<sup>8,14</sup> display lower permselectivity and higher permeability than polyimides, one of the materials that exhibit better gas separation performance.<sup>11</sup> Recently the need to investigate how the presence of imide groups in polynorbornenes could affect the permselectivity of membranes prepared from these materials has become evident. For this purpose we proceeded<sup>7,15</sup> with the synthesis and polymerization of *N*-(1-adamantyl)-*exo*-norbornene-5,6-dicarboximide, *N*-cyclohexyl-*exo*-nor-

bornene-5,6-dicarboximide, and *N*-phenyl-*exo*-norbornene-5,6-dicarboximide as well as the copolymers *N*-(1-adamantyl)-*exo*-norbornene-5,6-dicarboximide/norbornene, with molar compositions 70/30, 50/50, and 30/70. The permselectivity of these membranes was found to be dependent on the type of gases to be separated. For example, the permselectivity of oxygen with respect to nitrogen,  $\alpha(\text{O}_2/\text{N}_2)$ , is ca. 5.50 for membranes obtained from *N*-(1-adamantyl)-*exo*-norbornene-5,6-dicarboximide (50/50) copolymers. For the separation of  $\text{H}_2$  from  $\text{C}_2\text{H}_6$ , the membranes prepared from *N*-(1-adamantyl)-*exo*-norbornene-5,6-dicarboximide exhibit very good performance. In general, this study showed that the presence of imide groups enhances the permselectivity of polynorbornenes.

It is important to study how slight modifications in the structure of polymers may affect the gas transport properties of membranes prepared from them. In this work, we extended the preceding studies to the synthesis of *exo-N*-phenyl-7-oxanorbornene-5,6-dicarboximide (PhONDI), and its further copolymerization with norbornene (NB). Then we studied the transport characteristics of the membranes prepared from poly(*exo-N*-phenyl-7-oxanorbornene-5,6-dicarboximide-*co*-norbornene) (50/50) to different gases: hydrogen, argon, oxygen, nitrogen, carbon monoxide, carbon dioxide, methane, ethane, and ethylene. From permeation results, the permselectivity coefficients of the membranes for different pairs of gases were obtained and compared with the pertinent results reported for other polynorbornenes containing imide groups in the structure. Only sorption experiments of the most soluble gases were performed, specifically, carbon dioxide, ethane, ethylene, and methane, because the relatively small amount of copolymer available precluded the possibility of obtaining with enough precision the solubility coefficient of the less soluble gases.

## Experimental Section

**Materials.** *exo*-7-Oxanorbornene-5,6-dicarboxylic anhydride (*exo*-ONDA, **1**), norbornene, aniline, and other chemicals were purchased from Aldrich Chemical Co. Norbornene was distilled from sodium metal. 1,2-Dichloroethane and toluene were dried over anhydrous calcium chloride and distilled under nitrogen over CaH<sub>2</sub>. Catalyst **I**, 1,3-bis(2,4,6-trimethylphenyl)-4,5-dihydroimidazol-2-ylidene)(PCy<sub>3</sub>)Cl<sub>2</sub>Ru=CHPh,<sup>16</sup> was purchased from Stream Chemical Co. and used as received.

**Measurements.** <sup>1</sup>H NMR and <sup>13</sup>C NMR spectra were recorded with a Varian spectrometer at 300 and 75.5 MHz frequencies, respectively, in CDCl<sub>3</sub> with tetramethylsilane (TMS) as internal standard.

The glass transition temperature was measured under nitrogen with a Du Pont 2100 instrument, at a heating rate of 10 °C/min. The samples were encapsulated in standard aluminum DSC pans in duplicate. Each pan was run twice on the temperature range 30–200 °C. The glass transition temperature was taken as the temperature at which the baseline in the glassy region intercepts the straight line drawn through the middle point of the endotherm. FTIR spectra were obtained on a Nicolet 510p spectrometer.

Copolymer compositions were determined by <sup>1</sup>H NMR integration of the olefinic peak of *exo*-*N*-phenyl-7-oxanorbornene-5,6-dicarboximide (PhONDI) (6.15–5.85 ppm) units relative to the olefinic protons of norbornene units (5.34 ppm). Molecular weights and molecular weight distributions with reference to polystyrene standards were determined with a Varian 9012 GPC instrument at 30 °C in chloroform (universal column and a flow rate of 1 mL min<sup>-1</sup>).

Membranes were prepared by casting from chloroform solutions. Gas permeation was measured at 30 °C using a thermostated experimental device described in detail elsewhere.<sup>17</sup> Sorption experiments were performed in a thermostated experimental device made up of a reservoir chamber connected by a valve to the sorption chamber that contained the polymer in film form.<sup>18</sup> The reservoir and the sorption chambers were equipped, respectively, with Gometrics (0–35 bar) and MKS-722 (0–33 atm) pressure transducers. Gas at a given pressure was introduced into the reservoir chamber, and once it reached the temperature of interest, the valve separating the reservoir from the sorption chamber was suddenly opened and closed. The variation of the pressure of the gas by effect of the sorption process was recorded as a function of time in the sorption chamber. The leaks and the adsorption of gas in the walls of the latter chamber were previously measured in a blank experiment. The gas concentration in cm<sup>3</sup> of gas(STP)/cm<sup>3</sup> of polymer at the pressures and temperature of interest was obtained by means of the gas equation using the suitable compressibility coefficients.

**Monomer Synthesis.** *exo*-*N*-Phenyl-7-oxanorbornene-5,6-dicarboximide (PhONDI, **3**) was prepared according to the literature.<sup>19</sup> *exo*-ONDA **1** (5 g, 30 mmol) was dissolved in 17 mL of toluene. To the stirred solution of *exo*-ONDA 2.8 g of aniline (30 mmol) in 10 mL of toluene was added dropwise. The reaction was maintained at 40 °C for 2 h and then cooled to room temperature. A precipitate was filtered and dried to give 7.6 g (29 mmol) of amic acid. Obtained amic acid **2** (7.6 g, 29 mmol), anhydrous sodium acetate (1.12 g, 14 mmol), and acetic anhydride (23 g, 224 mmol) were heated at 70 °C for 3 h and then cooled. The solid crystallized on cooling was filtered, washed several times with water, and dried in a vacuum oven at 50 °C overnight. Pure monomer **3** (Figure 1) was obtained after twice recrystallization from methanol: yield = 89%, mp = 164–165 °C.

<sup>1</sup>H NMR (300 MHz, CDCl<sub>3</sub>): δ (ppm) = 7.49–7.26 (5H, m), 6.56 (2H, s), 5.39 (2H, s), 3.0 (2H, s).

<sup>13</sup>C NMR (75 MHz, CDCl<sub>3</sub>): δ (ppm) = 175.3, 136.6, 129.1, 128.7, 126.5, 81.3, 47.5.

FT-IR: 3064, 3021, 3003, 1775, 1715, 1595, 1496, 1380, 1287, 1186, 874, 713 cm<sup>-1</sup>.

**Monomer Metathesis Polymerization.** It was carried out in glass vials under a dry nitrogen atmosphere at room temperature. Adding benzaldehyde under a nitrogen atmo-

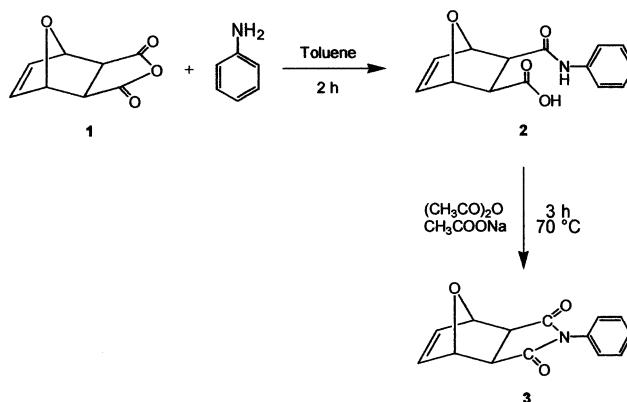


**Figure 1.** Synthesis route of *exo*-*N*-phenyl-7-oxanorbornene-5,6-dicarboximide (**3**).

sphere terminated the polymerization, and the solution was poured into an excess of methanol. The polymer was purified by solubilization in chloroform containing a few drops of 1 N HCl and precipitation into methanol, and it was further dried in a vacuum oven at 40 °C to constant weight.

**Synthesis of Copoly(*exo*-*N*-phenyl-7-oxanorbornene-5,6-dicarboximide/norbornene) (**4**).** One gram (4.15 mmol) of **3**, 0.40 g (4.15 mmol) of NB, and 0.0071 g (0.0084 mmol) of catalyst **I** were stirred in 8.4 mL of 1,2-dichloroethane at room temperature for 1 h. The polymer obtained (Figure 2) was soluble in chloroform and dichloromethane.

<sup>1</sup>H NMR (300 MHz, CDCl<sub>3</sub>): δ (ppm) = 7.47–7.25 (5H, m), 6.15 (2H, s, trans), 5.88 (2H, m, cis), 5.64 (2H, m, trans), 5.34 (2H, m, cis), 4.46 (2H, m), 3.35 (2H, m), 2.58 (2H, m), 2.44 (2H, s), 2.06–1.72 (2H, m), 1.60–1.0 (4H, m).

<sup>13</sup>C NMR (75 MHz, CDCl<sub>3</sub>): δ (ppm) = 174.6, 133.3, 132.5, 131.4, 129.1, 128.7, 126.3, 82.5, 52.6, 43.1, 40.6, 32.1.

FT-IR: 2997, 2940, 2854, 1775, 1716, 1555, 1498, 1376, 1308, 1178, 740, 691 cm<sup>-1</sup>.

The values of the number-average molecular weight,  $M_n$ , heterodispersity index,  $M_w/M_n$ , and glass transition temperature of poly(*exo*-*N*-phenyl-7-oxanorbornene-5,6-dicarboximide-co-norbornene) were, respectively,  $1.8 \times 10^5$ , 1.4, and 125 °C.

## Results

**Permeation Results.** An illustrative curve depicting the variation of the pressure of nitrogen with time in the downstream chamber is shown in Figure 3. As usual, a transitory appears at short times followed by a steady region at which the pressure is a linear function of time. The dependence of the pressure on time, calculated from the integration of Fick's second law assuming the diffusion coefficient constant,<sup>20</sup> is shown in Figure 3 for nitrogen. The good fitting between computed and experimental results suggests that the assumption  $D = \text{constant}$  holds. The same occurs for the other gases. The extrapolation of the steady-state region intercepts the abscissa axis at the "time lag"  $\theta$ .<sup>21</sup> The diffusion coefficient was obtained from  $D = L^2/6\theta$ , where  $L$  is the membrane thickness, whereas the permeability coefficient,  $P$ , was calculated from the permeation results in steady-state conditions.

Values at 30 °C of the permeability and diffusion coefficients for different gases are given in the second and third columns of Table 1, respectively. The results show that  $P(\text{H}_2) > P(\text{CO}_2) > P(\text{O}_2) > P(\text{Ar}) > P(\text{CO}) > P(\text{C}_2\text{H}_4) \cong P(\text{CH}_4) > P(\text{N}_2) > P(\text{C}_2\text{H}_6)$ , whereas the values of the diffusion coefficient follow the trend  $D(\text{H}_2) \gg D(\text{O}_2) > D(\text{Ar}) > D(\text{CO}_2) \cong D(\text{N}_2) > D(\text{CO}) > D(\text{CH}_4) > D(\text{C}_2\text{H}_4) > D(\text{C}_2\text{H}_6)$ . The results for the apparent solubility coefficient, obtained from the ratio  $P/D$ , are shown in the fourth column of Table 1. It can be seen

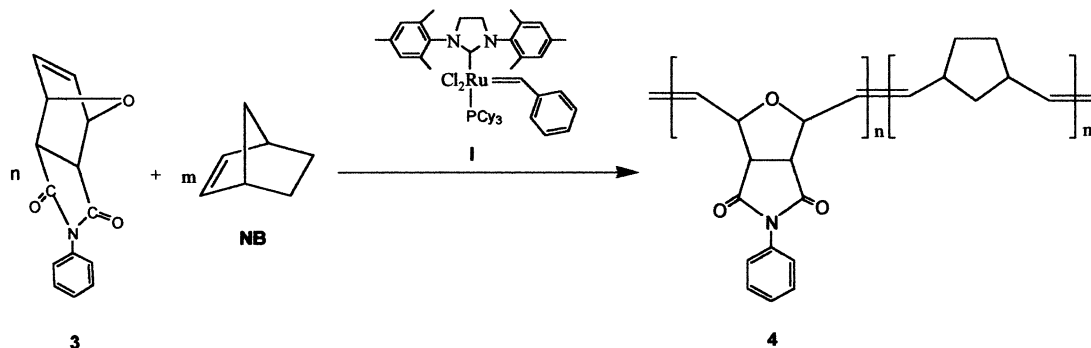


**Figure 2.** Scheme showing synthesis of poly(*exo*-*N*-phenyl-7-oxanorbornene-5,6-dicarboximide-*co*-norbornene) (50:50) via ROMP.

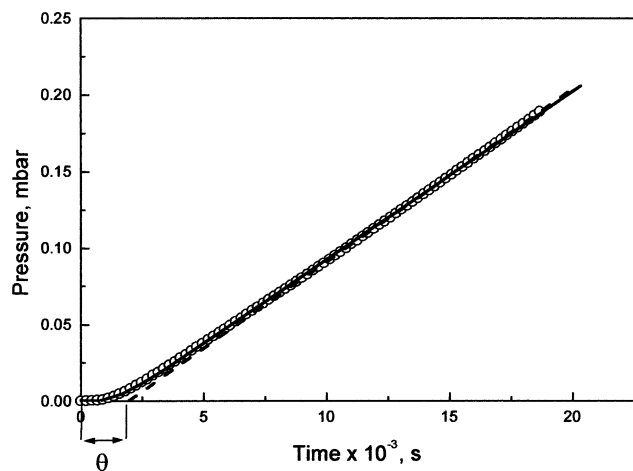


**Figure 3.** Dependence of the pressure of nitrogen in the downstream chamber on time, at 30 °C. Continuous line represents the isotherm calculated by integration of Fick's second law assuming the diffusion coefficient independent of concentration.

**Table 1. Permeation and Sorption Results for Different Gases at 30 °C and 1 atm Pressure**

gas	$P$ , barrers	$D \times 10^8$ , $\text{cm}^2/\text{s}$	$S \times 10^3$ , $\text{cm}^3(\text{STP})/\text{cm}^3$	$S \times 10^3$ , from sorption <sup>b</sup>
CO <sub>2</sub>	6.14	1.50	41.0	50.2
O <sub>2</sub>	0.99	3.94	2.5	
N <sub>2</sub>	0.21	1.42	1.5	
Ar	0.57	2.59	2.2	
CO	0.38	1.03	3.7	
H <sub>2</sub>	9.21	129	0.7	
CH <sub>4</sub>	0.27	0.62	4.3	7.9
C <sub>2</sub> H <sub>4</sub>	0.32	0.16	19.4	32.5
C <sub>2</sub> H <sub>6</sub>	0.22	0.06	37.8	26.4

<sup>a</sup>  $S = PD$ . <sup>b</sup> Units of  $S$ :  $\text{cm}^3$  of gas(STP)/( $\text{cm}^3$  of polymer cmHg).

that  $S(\text{CO}_2) > S(\text{C}_2\text{H}_4) > S(\text{C}_2\text{H}_6) > S(\text{CH}_4) > S(\text{CO}) > S(\text{O}_2) > S(\text{Ar}) > S(\text{N}_2) > S(\text{H}_2)$ . The small solubility coefficient of hydrogen in the membranes is responsible for the rather low flow rate of this gas across the membrane, only somewhat larger than that of carbon dioxide.

**Sorption Results.** Sorption experiments of carbon dioxide, methane, ethylene, and ethane were conducted by monitoring the decrease of pressure with time in a chamber containing the polymer in film form. Gas concentrations are represented as a function of pressure in Figure 4. The values of the solubility coefficients at 1 atm of CO<sub>2</sub>, CH<sub>4</sub>, C<sub>2</sub>H<sub>4</sub>, and C<sub>2</sub>H<sub>6</sub>, obtained at 30 °C from sorption measurements, are given in the fifth column of Table 1, while those obtained from permeation experiments appear in the fourth column. As often is the case, there are small differences between the

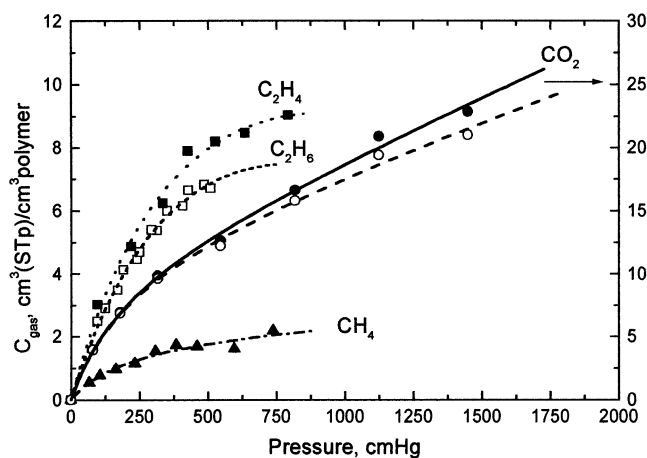


**Figure 4.** Isotherms at 30 °C representing the sorption of CO<sub>2</sub>, C<sub>2</sub>H<sub>4</sub>, C<sub>2</sub>H<sub>6</sub>, and CH<sub>4</sub> as a function of pressure. The dashed isotherm for CO<sub>2</sub> represents the concentration of this gas in the membrane calculated assuming ideal gas behavior.

**Table 2. Values of Henry's Law Solubility Constant and Langmuir Parameters for Carbon Dioxide, Methane, Ethylene, and Ethane at 30 °C and 1 atm Pressure**

gas	$k_D \times 10^3$ , $\text{cm}^3(\text{STP})/(\text{cm}^3 \text{cmHg})$	$C_H$ , $\text{cm}^3(\text{STP})/\text{cm}^3$	$b \times 10^3$ , $(\text{cmHg})^{-1}$
CO <sub>2</sub>	9.4	7.9	8.5
CH <sub>4</sub>	0.8	1.8	5.4
C <sub>2</sub> H <sub>4</sub>	3.4	8.8	4.4
C <sub>2</sub> H <sub>6</sub>	3.5	8.1	3.6

results obtained by both techniques though they follow the same trend, that is,  $S(\text{CO}_2) > S(\text{C}_2\text{H}_4) > S(\text{C}_2\text{H}_6) > S(\text{CH}_4)$ .

As usual, the isotherms display concavity with respect to the abscissa axis observed in the sorption curves of most glassy systems. The dual-mode model, which assumes the glassy state as formed by a continuous phase where microcavities accounting for the excess volume are dispersed, has traditionally been used to interpret gas sorption in glassy polymers. The solubility in the continuous phase obeys Henry's law, while the microcavities act like Langmuir sites in which adsorption processes take place.<sup>22,23</sup> As shown in Figure 4, the sorption results fit rather well those predicted by the dual-mode model using the values given in Table 2 for the absorption Henry's constant,  $k_D$ , the Langmuir capacity,  $C_H$ , and the Langmuir affinity parameter,  $b$ . An inspection of the values of these parameters indicates that the gas concentration in Langmuir sites follows the trend: C<sub>2</sub>H<sub>4</sub>  $\cong$  CO<sub>2</sub>  $\cong$  C<sub>2</sub>H<sub>6</sub> > CH<sub>4</sub>. In any case, the value of  $C_H$  for CO<sub>2</sub> is significantly lower than that reported for polynorbornenes and fluorine-containing polynorbornenes.<sup>9</sup>

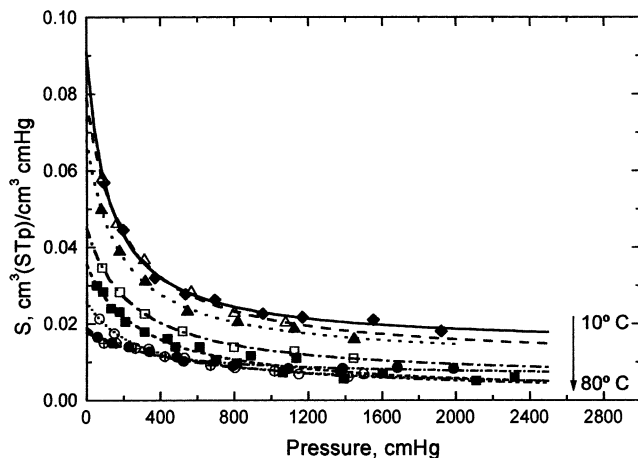


**Figure 5.** Isotherms showing the dependence of the solubility coefficient of CO<sub>2</sub> on pressure at different temperatures.

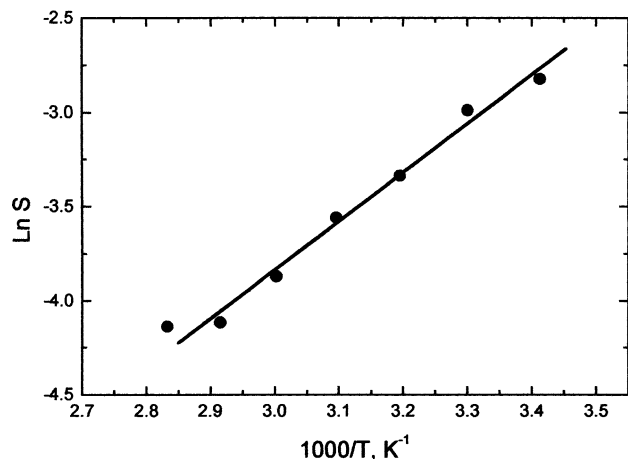


**Figure 6.** Arrhenius plots for the solubility coefficient of CO<sub>2</sub>.

The results for the solubility coefficient of CO<sub>2</sub> at different temperatures, plotted as a function of pressure in Figure 5, show that  $S$  undergoes a sharp decrease at low pressures, remaining nearly constant at pressures higher than 10 atm.. Moreover, the decrease of the solubility coefficient is lower, the higher the temperature is. As shown in Figure 6, the temperature dependence of the solubility coefficient follows Arrhenius behavior and the value of the sorption heat obtained from the Arrhenius plot is  $-5.2 \text{ kcal mol}^{-1}$  at 1 atm. Therefore, the solution of CO<sub>2</sub> in the membranes is an exothermic process, as occurs with the solubility of most gases in glassy polymers.<sup>24</sup> Arrhenius plots for the Henry's constant,  $k_D$ , the gas concentration at the Langmuir sites,  $C_H$ , and the affinity parameter,  $b$ , are shown in Figure 7. The activation energies amount to  $-6.6$ ,  $-4.1$ , and  $-1.2 \text{ kcal mol}^{-1}$  for  $k_D$ ,  $b$ , and  $C_H$ , respectively.

### Discussion

The dual-mode model suggests that the Langmuir capacity of glassy membranes depends on  $T_g - T$ .<sup>25,26</sup> According to this approach, a plot of  $v_g C'_H / (\alpha_g - \alpha_l)$  vs  $T_g - T$  for glassy membranes should give a straight line passing through the origin. Notice that  $\alpha_g$  and  $\alpha_l$  are, respectively, the thermal expansion coefficient of the glass and the liquid at temperature  $T$  and  $v_g$  is the specific volume. Therefore, the relatively low value of  $C_H$  found for the membranes used in this study may be due to the closeness of the  $T_g$  of copoly(*exo-N*-phenyl-

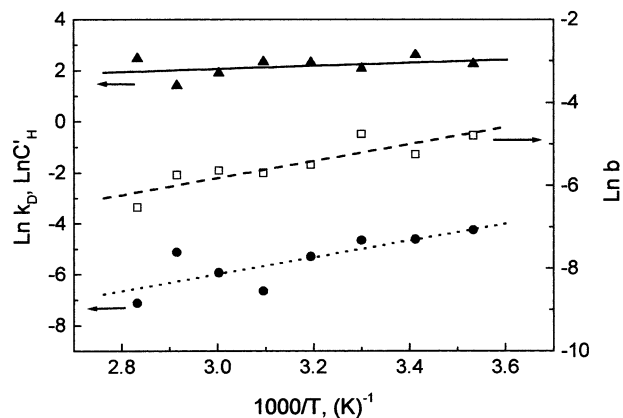


**Figure 7.** Arrhenius plots for the parameters of the dual-mode model of carbon dioxide: (●)  $k_D$ , (□)  $b$  and (▲)  $C_H$ .

7-oxanorbornene-5,6-dicarboximide/norbornene) to the working temperature.

By assuming that the continuous phase in the dual-mode model behaves like a liquid, the solubility Henry's constant can be obtained from the variation of the chemical potential of the gas in the liquid state dissolved in the polymer. The Flory–Huggins theory,<sup>27</sup> in conjunction with the Clausius–Clapeyron equation that allows for the determination of the vapor pressure of the gas in the liquid form at the temperature of interest, leads to the following expression for Henry's constant<sup>28,29</sup>

$$k_D = \frac{22414}{76\bar{V}} \exp\left[-(1 + \chi) - \frac{\lambda}{RT_b}\left(1 - \frac{T}{T_b}\right)\right] \quad (1)$$

where  $T_b$  is the boiling temperature of the gas at 1 bar,  $\lambda$  is the latent heat of vaporization at  $T_b$ ,  $\chi$  is an enthalpic parameter that accounts for the polymer–gas interaction and  $\bar{V}$  is the partial molar volume of the gas in cm<sup>3</sup>/mol. According to eq 1, the higher  $T_b$  is and/or the lower  $\chi$  is, the higher the value of the Henry's constant is. As shown in Table 3, a good concordance between the experimental and calculated values of  $k_D$  is obtained using the reasonable values of the interaction parameter given in the fifth column of this table. This is a remarkable fact considering that in the development of eq 1 not only the Flory–Huggins theory was used that, in principle, is only valid for rubbery polymers, but also a rather wide extrapolation interval of temperature was used to obtain the vapor pressure of the gas by means of the Clausius–Clapeyron equation. It should be pointed out that the molar partial volume used in the calculations was that corresponding to  $T_b$  at 1 bar. To use the true value of  $\bar{V}$  at 30 °C only would slightly alter the results obtained for  $\chi$ .

Occasional fluctuations in the glassy state give rise to the formation of channels through which the diffusant molecule may slip to a nearby cavity. The possibility of slippage requires not only a suitable velocity of the molecule when the fluctuation takes place but also the radius of the channel to be larger than the radius of the diffusant. The size of the molecule of a gas can be estimated from the Lennard-Jones collision diameter  $\sigma_c$ , determined on the basis of the molecular interactions of a gas, and the kinetic diameter which is close to the molecular sieving dimension of the molecule.<sup>30,31</sup> The collision and kinetic diameters are, respectively, widely accepted correlation parameters for diffusivity in the rubbery and glassy states. The values of the natural

**Table 3. Values of the Enthalpic Parameter That Accounts for the Interaction Polymer Gas, at 30 °C**

gas	$T_b$ , °C	$\lambda$ , kcal mol <sup>-1</sup>	$\bar{V}_i^a$ , cm <sup>3</sup> /mol	$\chi$	$10^3 \times k_{D, \text{calcd}}$ , cm <sup>3</sup> (STP)/(cm <sup>3</sup> cmHg)	$10^3 \times k_{D, \text{expt}}$ , cm <sup>3</sup> (STP)/(cm <sup>3</sup> cmHg)
CO <sub>2</sub>	-78.5	6.06	46	0	8.6	9.4
CH <sub>4</sub>	-159	2.21	38	2	0.9	0.8
C <sub>2</sub> H <sub>6</sub>	-88.6	3.51 <sup>b</sup>	55	2.5	3.8	3.5
C <sub>2</sub> H <sub>4</sub>	-103.7	3.23 <sup>b</sup>	49.4	2.5	2.6	3.4

<sup>a</sup> Molar partial volume at  $T_b$ . <sup>b</sup> Reference 32.

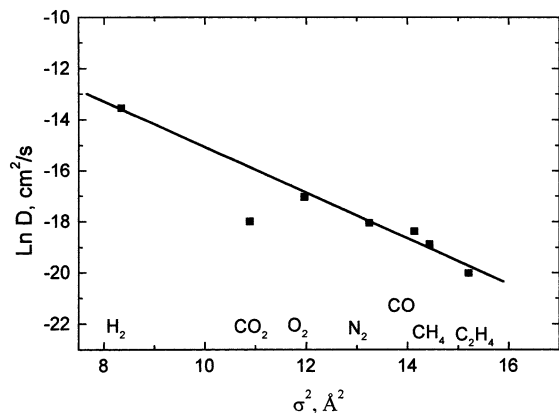


**Figure 8.** Plot of natural logarithm of the diffusion coefficient against the square of the kinetic diameter of different gases indicated in the figure.

logarithm of the diffusion coefficients of H<sub>2</sub>, N<sub>2</sub>, CO, Ar, O<sub>2</sub>, CH<sub>4</sub>, C<sub>2</sub>H<sub>4</sub>, and C<sub>2</sub>H<sub>6</sub>, represented as a function of the square of the kinetic diameter in Figure 8, fit rather well to a straight line. It is worth noting that the diffusion coefficient of carbon dioxide falls well below the straight line, suggesting that some kind of polymer-gas interaction hindering the diffusive process occurs. The high solubility of CO<sub>2</sub> and the anomalous low diffusion coefficient of this gas may be related to the polarity of the imide groups. CO<sub>2</sub> is a nonpolar molecule, but it still has a strong quadrupole moment that makes possible dipole-dipole interaction with the imide groups. These interactions may enhance solubility, but severely hinder diffusant motions.

The rather low permeability coefficient of the membranes, despite the relatively bulky side groups of the monomer containing imide groups, could be caused by the stereochemical compositions of polynorbornene chains. It is well-known<sup>32,33</sup> that materials obtained by ROMP may give rise to the formation of blocks of *cis* and/or *trans* configurations having different specific chain lengths. The incompatibility between blocks could result in microphase separation that increases the tortuosity of the diffusive path, thus decreasing the diffusion coefficient.

The separation or selectivity factor for two gases A and B can be written as

$$\alpha(A/B) = \frac{P(A)}{P(B)} = \frac{D(A) S(A)}{D(B) S(B)} \quad (2)$$

Equation 2 indicates that the discriminative effects to gas transport in membranes may be governed by the diffusive step, the sorption process, or both. In general, polynorbornene is characterized for having rather low permeability accompanied by low permselectivity. For example, the value of  $\alpha(\text{O}_2/\text{N}_2)$  for polynorbornene<sup>9</sup> is only 1.9, significantly lower than the value of 5 or larger reported for polyimides, polysulfones, etc.<sup>1</sup> An increase in the tacticity of polynorbornene has proved to enhance

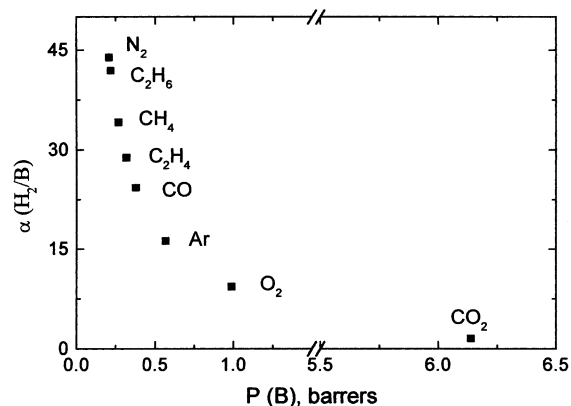


**Figure 9.** Experimental separation factor of hydrogen with respect to different gases as a function of the permeability coefficients of the latter.

the permselectivity of the membranes prepared from these polymers.<sup>12</sup> Also, introduction of fluorine atoms in the main chain or in side groups as well as the attachment of organosilicon moieties to polynorbornene seems to increase the permeability without detriment to the selectivity.

It is worth noting that  $\alpha(\text{H}_2/\text{CO}_2) \cong 1.5$  for poly(*exo-N*-phenyl-7-oxanorbornene-5,6-dicarboximide-*co*-norbornene) membranes in spite of the fact that  $D(\text{H}_2)/D(\text{CO}_2) = 86$ . In this case, however, the low solubility of hydrogen in comparison with that of carbon dioxide is responsible for the poor discriminative properties of the membrane for the separation of hydrogen from carbon dioxide.

The performance of the membranes described in this work for separation of hydrogen from N<sub>2</sub>, O<sub>2</sub>, Ar, CO, CO<sub>2</sub>, CH<sub>4</sub>, C<sub>2</sub>H<sub>4</sub>, and C<sub>2</sub>H<sub>6</sub> is depicted in Figure 9. The values of  $\alpha(\text{H}_2/B)$  represented in terms of increasing values of the permeability coefficient of B gives a curve that shows a strong decrease of the separation coefficient with increasing values of  $P(B)$ . The values of  $\alpha(\text{H}_2/\text{N}_2)$ ,  $\alpha(\text{H}_2/\text{CH}_4)$ , and  $\alpha(\text{H}_2/\text{C}_2\text{H}_6)$  are significantly higher than those reported for poly(vinyltrimethylsilylnorbornene) and fluorine-containing ring-opened polynorbornenes.<sup>9</sup> However, the permselectivity factors depicting the separation of hydrogen from the other gases are on average similar to those reported for membranes of poly[(1-adamantyl)-*exo*-norbornene-5,6-dicarboximide] and poly(*N*-cyclohexyl-*exo*-norbornene-5,6-dicarboximide) as well as for copolymers of *N*-(1-adamantyl)-*exo*-norbornene-5,6-dicarboximide/norbornene, with molar compositions 70/30, 50/50, and 30/70.<sup>15</sup>

The membranes exhibit a separation factor  $\alpha(\text{O}_2/\text{N}_2) = 4.7$ , somewhat higher than that reported for the membranes prepared from polynorbornenes containing imide functions in their structure, with the exception of the copolymer (1-adamantyl)-*exo*-norbornene-5,6-dicarboximide/norbornene (50/50), for which  $\alpha(\text{O}_2/\text{N}_2) = 5.5$ .<sup>16</sup>

## Conclusions

The synthesis of poly(*exo-N*-phenyl-7-oxanorbornene-5,6-dicarboximide-*co*-norbornene) is reported. The Langmuir capacity of the most condensable gases in membranes of this polymer prepared by casting is relatively low, as one would expect from the relatively low glass transition temperature of the copolymer. The membranes exhibit pretty good properties to separate hydrogen from other gases such as nitrogen, methane, ethylene, and ethane, in comparison with other membranes prepared from norbornenes containing fluorine atoms or organosilicon moieties.

A shortcoming of these membranes is their low permeability presumably caused by either the good packing of the chains or by the increase in the tortuosity of the diffusive path arising from the possible existence of segregate stereoregular blocks of *cis* and *trans* configurations. It would be important to increase the permeability of the membranes either by using polymerization methods that enhance the stereoregularity of the chains or by fluorinating or introducing organosilicon moieties in norbornenes containing imide groups in the structure.

**Acknowledgment.** We thank the CONACyT for generous support of this research with Contract No. NC-204. The authors thank Miguel Angel Canseco, Juan Manuel Garcia Leon, and Gerardo Cedillo for their assistance in thermal, GPC, and NMR analyses. Support of this work by the CAM (Spain) through Grant Bio-009-2000 is also gratefully acknowledged.

## References and Notes

- (1) Kesting, R. E.; Fritzsche, A. K. *Polymeric Gas Separation Membranes*; Wiley-Interscience: New York, 1993.
- (2) Ohya, H.; Kudryavtsev, V. V.; Semenova, S. I. *Polyimide Membranes*; Gordon and Breach Publishers: Tokyo, 1996.
- (3) Tlenkopatchev, M. A.; Fomine, S.; Miranda, E.; Fomina, L.; Ogawa, T. *Polym. J.* **1995**, *27*, 1173.
- (4) Tlenkopatchev, M. A.; Fomine, S.; Fomina, L.; Gaviño, R.; Ogawa, T. *Polym. J.* **1997**, *29*, 622.
- (5) Maya, V. G.; Contreras, A. P.; Canseco, M. A.; Tlenkopatchev, M. A. *React. Funct. Polym.* **2001**, *49*, 145.
- (6) Asrar, J. *Macromolecules* **1992**, *25*, 5150.
- (7) Contreras, A. P.; Cerda, A. M.; Tlenkopatchev, M. A. *Macromol. Chem. Phys.* **2002**, *203*, 1811.
- (8) Finkelshtein, E. Sh.; Gringolts, M. L.; Ushakov, N. V.; Lakhtin, V. G.; Sloviev, S. A.; Yampol'skii, Yu. P. *Polymer* **2003**, *44*, 2483.
- (9) Yampol'skii, Yu. P.; Bepalova, N. B.; Finkelshtein, E. Sh.; Bondar, V. I.; Popov, A. V. *Macromolecules* **1994**, *27*, 2872.
- (10) Finkelshtein, E. Sh.; Makovetskii, K. L.; Yampol'skii, Yu. P.; Portnykh, E. B.; Ostrovskaja, I. Ya.; Kaliuzhnyi, N. E.; Pritula, N. A.; Gol'berg, A. I.; Yatsenko, M. S.; Plate, N. A. *Makromol. Chem.* **1991**, *192*, 1.
- (11) Bondar, V. I.; Kukharskii, Yu. M.; Yampol'skii, Yu. P.; Finkelshtein, E. Sh.; Makovetskii, K. L. *J. Polym. Sci., Part B: Polym. Phys.* **1993**, *31*, 1273.
- (12) Steinhäusler, T.; Koros, W. J. *J. Polym. Sci., Part B: Polym. Phys.* **1997**, *35*, 91.
- (13) Contreras, A. P.; Tlenkopatchev, M. A.; Ogawa, T.; Nakagawa, T. *Polym. J.* **2002**, *34*, 49.
- (14) Yampol'skii, Yu. P.; Shishatskii, S.; Alentiev, A.; Loza, K. *J. Membr. Sci.* **1998**, *149*, 203.
- (15) Contreras, A. P.; Tlenkopatchev, M. A.; López-González, M. M.; Riande, E. *Macromolecules* **2002**, *35*, 4677.
- (16) Scholl, M.; Ding, S.; Lee, C. W.; Grubbs, R. H. *Org. Lett.* **1999**, *1*, 953.
- (17) Laguna, M. F.; Saiz, E.; Guzmán, J.; Riande, E. *Macromolecules* **1998**, *31*, 7488.
- (18) Saiz, E.; López-González, M. M.; Riande, E.; Guzmán, J.; Compañ, V. *Phys. Chem. Chem. Phys.* **2003**, *5*, 2862.
- (19) Anderson, W. K.; Milowsky, A. S. *J. Org. Chem.* **1985**, *50*, 5423.
- (20) Crank, J. *The Mathematics of Diffusion*; Oxford University Press: New York, 1975.
- (21) Barrer, R. M. *Trans. Faraday Soc.* **1939**, *35*, 628.
- (22) Vieth, W. R.; Sladek, K. J. *J. Colloid Sci.* **1965**, *20*, 1014.
- (23) Reference 2, p 60.
- (24) van der Vegt, N. F. A. *J. Membr. Sci.* **2002**, *205*, 125.
- (25) Koros, W. J.; Paul, D. R. *J. Polym. Sci., Polym. Phys. Ed.* **1978**, *16*, 1947.
- (26) Muruganandam, N.; Koros, W. J.; Paul, D. R. *J. Polym. Sci., Part B: Polym. Phys.* **1987**, *25*, 1999.
- (27) Flory, P. J. *Principles of Polymer Chemistry*; Cornell University Press: Ithaca, NY, 1953; Chapter 21.
- (28) Petropoulos, J. H. *Pure Appl. Chem.* **1993**, *65*, 219.
- (29) Compañ, V.; López-González, M. M.; Riande, E. *Macromolecules*, in press.
- (30) Breck, D. W. *Zeolite Molecular Sieves*; Wiley-Interscience: New York, 1974; p 636.
- (31) Costello, L. M.; Koros, W. J. *J. Polym. Sci., Part B: Polym. Phys.* **1994**, *32*, 701.
- (32) Ivin, K. J.; Mol, J. C. *Olefin Metathesis and Metathesis Polymerization*; Academic Press: San Diego, CA, 1997.
- (33) Reid, R. C.; Prausnitz, J. M.; Poling, B. E. *The Properties of Gases and Liquids*, 4th ed.; McGraw-Hill: New York, 1987.

MA030285A